Article:
Blackburn, T. G., Ilderton, A., Marklund, M. et al. (1 more author) (2019) Reaching supercritical field strengths with intense lasers. New Journal of Physics. 053040. ISSN 1367-2630

https://doi.org/10.1088/1367-2630/ab1e0d

New Journal of Physics
The open access journal at the forefront of physics

Deutsche Physikalische Gesellschaft DPG IOP Institute of Physics

PAPER • OPEN ACCESS

Reaching supercritical field strengths with intense lasers

To cite this article: T G Blackburn *et al* 2019 *New J. Phys.* **21** 053040

New Journal of Physics
The open access journal at the forefront of physics

Deutsche Physikalische Gesellschaft DPG
IOP Institute of Physics

Published in partnership with: Deutsche Physikalische Gesellschaft and the Institute of Physics

OPEN ACCESS

RECEIVED
24 January 2019

REVISED
23 April 2019

ACCEPTED FOR PUBLICATION
30 April 2019

PUBLISHED
29 May 2019

PAPER

Reaching supercritical field strengths with intense lasers

T G Blackburn[1,4], A Ilderton[2], M Marklund[1,4] and C P Ridgers[3]

[1] Department of Physics, Chalmers University of Technology, SE-41296 Gothenburg, Sweden
[2] Centre for Mathematical Sciences, University of Plymouth, Devon PL4 8AA, United Kingdom
[3] York Plasma Institute, Department of Physics, University of York, York, YO10 5DD, United Kingdom
[4] Present address: Department of Physics, University of Gothenburg, SE-41296 Gothenburg, Sweden.

E-mail: tom.blackburn@physics.gu.se

Keywords: radiation reaction, strong-field quantum electrodynamics (QED), radiative corrections

Abstract

It is conjectured that all perturbative approaches to quantum electrodynamics (QED) break down in the collision of a high-energy electron beam with an intense laser, when the laser fields are boosted to 'supercritical' strengths far greater than the critical field of QED. As field strengths increase toward this regime, cascades of photon emission and electron–positron pair creation are expected, as well as the onset of substantial radiative corrections. Here we identify the important role played by the collision angle in mitigating energy losses to photon emission that would otherwise prevent the electrons reaching the supercritical regime. We show that a collision between an electron beam with energy in the tens of GeV and a laser pulse of intensity 10^{24} W cm^{-2} at oblique, or even normal, incidence is a viable platform for studying the breakdown of perturbative strong-field QED. Our results have implications for the design of near-term experiments as they predict that certain quantum effects are enhanced at oblique incidence.

1. Introduction

Experimental exploration of nonperturbative quantum electrodynamics (QED) is challenging as it requires electromagnetic fields comparable in strength to the critical field of QED $E_{\rm cr} = 1.3 \times 10^{18}$ V m^{-1}, the field strength which induces electron–positron pair creation from the vacuum itself [1, 2]. Nevertheless, ever-increasing laser intensities [3–5] make it possible to probe fields that are effectively supercritical, i.e. that have magnitude greater than $E_{\rm cr}$. This is achieved using the Lorentz boost when ultrarelativistic electrons collide with an intense laser pulse [6, 7], as the parameter χ_e that controls the importance of nonlinear QED is the rest-frame electric field normalised to the critical field strength $E_{\rm cr} = m^2/e$. χ_e is covariantly expressed as $\chi_e = |F_{\mu\nu}u^\nu|/E_{\rm cr}$ [8], where F is the electromagnetic field tensor and u the electron four-velocity. We use natural units in which $\hbar = c = 1$ (e is the elementary charge, m the electron mass) throughout.

In the supercritical regime $\chi_e \gg 1$, particle dynamics is dominated by cascades of photon emission and electron–positron pair creation [8–11]. The importance of studying these phenomena is motivated by their relevance to high-field astrophysical environments, such as magnetars [12–14], and to laser-matter interactions beyond the current intensity frontier [15, 16]. It is also of considerable theoretical interest, as when $\alpha\chi_e^{2/3}$ approaches unity (α is the fine-structure constant), it is conjectured that radiative corrections to quantum processes become so large that all current, perturbative, predictions fail [17, 18] and strong-field QED becomes fully nonperturbative.

In this article we show how the collision of an intense laser pulse with an ultrarelativistic electron beam may be used to probe the supercritical regime. A significant obstacle to this is posed by radiation reaction, an accelerating charge's loss of energy to photon emission, which strongly reduces u at $\chi_e \gg 1$, thereby suppressing χ_e itself [19–22]. We show that this can be mitigated by appropriate choice of the angle at which the beams collide. We present a theoretical expression for the maximum χ_e, which predicts, contrary to the expectation that the ideal geometry is counterpropagation, that oblique incidence is favoured for laser pulses of high intensity or long duration. This enhances certain quantum effects on radiation reaction, namely straggling

[23, 24] and stochastic broadening [25]. As a result, not only will laser-electron collision experiments that are practically constrained to oblique incidence [26] still detect signatures of quantum effects, but these signatures can be stronger than they would be in a head-on collision. Furthermore, we show that at the intensity and electron energy necessary to probe radiative corrections, oblique, or even normal, incidence is strongly favoured to reduce radiative losses that would otherwise prevent reaching such high χ_e.

2. Effect of radiative losses on the maximum χ_e

High-power lasers compress energy into ultrashort pulses that can be focussed almost to the diffraction limit. The theoretical upper bound on χ_e is obtained by treating the laser as a pulsed plane electromagnetic wave with peak dimensionless amplitude $a_0 = eE_0/(m\omega_0)$, peak electric field strength E_0 and central frequency ω_0, and neglecting radiative losses. Then

$$\chi_e = \frac{a_0\gamma_0\omega_0(1 + \cos\theta)}{m}, \tag{1}$$

where θ is the collision angle (defined to be zero for counterpropagation) and $\gamma_0 \gg 1$ is the initial Lorentz factor of the electron. The largest possible quantum parameter is $\chi_0 = \chi_e(\theta = 0)$.

Experiments at $a_0 \simeq 0.4$, $\chi_e \simeq 0.3$ have demonstrated nonlinear QED effects including pair creation [6, 7], and recently evidence of radiation reaction has been reported at $a_0 \simeq 10$, $\chi_e \simeq 0.1$ [27, 28]. At present, the highest field strengths are equivalent to $a_0 \simeq 50$ [29, 30], or $\chi_0 \simeq 1$ at $\gamma_0 m \simeq 1$ GeV; $a_0 > 100$ is expected in the next generation of laser facilities [31–33]. The stronger the electromagnetic field, the lower the electron energy that is needed to reach high χ_e. In experiments with aligned crystals where the field strength $\sim 10^{13}$ V m^{-1} [34], $\chi_e \simeq 1$ and evidence of quantum radiation reaction require 100 GeV electron beams [35]. Earlier experiments achieved higher $\chi_e \simeq 7$ with the use of tungsten, rather than silicon, targets due to the stronger nuclear field [36]. $\chi_e > 1$ will also be probed in beam–beam interactions in the next generation of linear colliders [37, 38].

Despite the strong spatial and temporal compression of laser pulses, it is inevitable that the electron will have to traverse a finite region of space over which the field strength ramps up before it reaches the point of peak a_0. If significant energy loss takes place during this interval, the electron's χ_e will be much smaller than that predicted by (1). We now derive a scaling for the maximum χ_e reached by an electron, which accounts for radiative losses and the spatial structure of the laser pulse, following [39].

2.1. Scaling law

Consider an electron colliding at angle θ with a linearly polarised laser pulse that has Gaussian temporal and radial intensity profiles of size τ and r_0 respectively. Here τ is the full width at half maximum of the temporal intensity profile and r_0 is the waist of the focussed pulse (the radius at which the intensity falls to $1/e^2$ of its peak). As the crossing angle θ is not necessarily zero, we must take the transverse structure of a focussed laser pulse into account. In our Monte Carlo simulations, the spatial dependence of the electromagnetic field is treated as a tightly focussed Gaussian beam with waist size r_0 and Rayleigh length $z_R = \pi r_0^2/\lambda$. The fields are calculated up to fourth-order in the diffraction angle r_0/z_R, following [40], and therefore go beyond the paraxial approximation. Nevertheless, in order to obtain a relatively simple analytical expression for the maximum χ_e, we use a reduced model for the fields that will, as we show, capture the essential physics.

The laser pulse is treated as a 'light bullet', with Gaussian temporal and transverse spatial profiles of constant size. We also neglect the longitudinal components of the fields and wavefront curvature, such that the pulse becomes a plane electromagnetic wave. For all the waist sizes under consideration (generally at least $r_0 = 2.5\lambda$, where λ is the wavelength), the transverse components provide the dominant contribution to χ_e. We assume that the electron Lorentz factor $\gamma \gg a(\phi)$, where $a(\phi) = eE(\phi)/(m\,\omega_0)$, the local value of the normalised electric field E at phase ϕ, at least up to the point where its quantum parameter is maximised. This occurs before the electron has undergone substantial energy losses, after which ponderomotive forces can eject the electron from the laser pulse at large angle [41], and our assumption that the trajectory is ballistic breaks down.

Under these circumstances, the envelope of the normalised electric field along the electron trajectory is given by $a(x, y, z, t) \simeq a_0 \exp[-(x^2 + y^2)/r_0^2 - 2\ln 2(t - z)^2/\tau^2]$, and $x = -t\sin\theta, y = 0, z = -t\cos\theta$. Here we have used the fact that the plane in which the collision angle lies may be chosen arbitrarily. This is written more compactly as [39, 42]

$$a(\phi) = a_0 \exp[-\ln(2)\phi^2/(2\pi^2 n_{\rm eff}^2)], \tag{2}$$

$$n_{\rm eff} = \frac{\omega_0\tau}{2\pi}\left[1 + \frac{\tau^2\tan^2(\theta/2)}{r_0^2\ln 4}\right]^{-1/2}, \tag{3}$$

defining the phase $\phi = (1 + \cos\theta)\omega_0 t$ and an effective duration (per wavelength) $n_{\rm eff}$. Carrier envelope phase effects may be neglected, as done here, provided $n_{\rm eff} \gtrsim 2$. The point at which χ_e is maximised is defined by $[\gamma(\phi)a(\phi)]' = 0$, where primes denote differentiation with respect to phase.

We substitute into this extremization condition: the $a(\phi)$ and $a'(\phi)$ given by (2); and $\gamma'(\phi) = \mathcal{P}/[2(1 + \cos\theta)m\omega_0]$, where $\mathcal{P} = 2\alpha m^2\chi_e^2 g(\chi_e)/3$ is the instantaneous radiated power (per unit time). The Gaunt factor $0 < g(\chi_e) \leqslant 1$ accounts for quantum corrections to the photon spectrum that reduce the the radiated power from its classically predicted value [9]; the factor of $\frac{1}{2}$ in $\gamma'(\phi)$ comes from averaging over the $\sin^2$ oscillation of the electric field (recall that (2) defines the envelope of the field and the pulse is linearly polarised). Then factors of ϕ are traded for χ_e using $\chi_e(\phi) = \gamma(\phi)a(\phi)\omega_0(1 + \cos\theta)/m$. The remaining dependence on $\gamma(\phi)$ is removed by setting $\gamma(\phi) = \gamma_0$, the electron's initial Lorentz factor.

This is motivated by the probabilistic nature of radiation losses in the quantum regime, which means that $\chi_e(\phi)$ is not single-valued at a given phase. Instead, there is a distribution $f(\chi_e, \phi)$ that evolves as the electron population travels through the laser pulse. The highest χ_e is reached by electrons that lose less energy than would be expected classically. This phenomenon is called 'straggling' [23, 43], or 'quenching' in pulses so short that it is possible that the electron does not radiate at all [44]. Such electrons are less affected by ponderomotive deflection as their energy remains large, which supports our assumption that the trajectory remains approximately ballistic at least up to the point at which χ_e is maximised. As our scaling is concerned with this part of the electron distribution function, setting $\gamma = \gamma_0$ is a way to isolate these electrons.

We find that maximum quantum parameter $\chi_{\rm max}$ satisfies

$$\frac{\chi_{\rm max}^4\, g^2(\chi_{\rm max})}{\chi_0^4} = \frac{9\ln 2(1 + \cos\theta)^2}{(\pi R_c n_{\rm eff})^2} \ln\left[\frac{(1 + \cos\theta)\chi_0}{2\chi_{\rm max}}\right]. \tag{4}$$

Here χ_0 is the largest possible quantum parameter ((1) with $\theta = 0$) and the classical radiation reaction parameter $R_c = \alpha a_0 \chi_0$ [20, 45].

In the limit $\chi_{\rm max} \ll 1$, (4) has a solution in terms of the Lambert function $\mathscr{W}$, which is defined for real $x > 0$ by $x = \mathscr{W}(x)\exp[\mathscr{W}(x)]$:

$$\frac{\chi_{\rm max}}{\chi_0} = \frac{1 + \cos\theta}{2} \mathrm{e}^{-\mathscr{W}(\delta^2)/4}, \tag{5a}$$

$$\delta = \frac{\pi R_c n_{\rm eff}(1 + \cos\theta)}{3\sqrt{2\ln 2}}. \tag{5b}$$

$\mathscr{W}(\delta^2)$ is strictly increasing for $\delta \geqslant 0$ and therefore χ_e decreases with increasing δ. Unlike (1), (5*a*) does not depend symmetrically upon a_0 and γ_0, as $\delta \propto a_0^2\gamma_0$. Hence it is more beneficial to increase γ_0 than a_0 when aiming for very large χ_e. Physically this is because the photon emission rate has a stronger dependence on a_0 than on γ_0; by minimising the number of emitted photons we also mitigate the radiative losses that would reduce χ_e. Indeed, $\chi_{\rm max}$ is generally smaller than χ_0 because it is reached in the rising edge of the pulse, before the electron encounters the point of highest intensity [39]. Compare (1) and (5*a*): the scaling of $\chi_{\rm max}$ with a_0 is much weaker in the latter case, because peak value of a_0 does not contribute fully.

2.2. Comparison to Monte Carlo simulations

To show that (4) can be used as a quantitative prediction of the largest χ_e that is reached in a laser-electron beam collision, we compare its predictions to the results of single-particle Monte Carlo simulations. These model a QED cascade of photon emission and pair creation by factorising it into a product of first-order processes [46, 47], which occur along the particles' classical trajectories at positions determined by integration of QED probability rates that are calculated in the locally constant field approximation [8]. This 'semiclassical' approach is valid when $a_0^3/\chi_e \gg 1$ because the formation lengths of the photons and electron–positron pairs are much smaller than the laser wavelength and interference effects are suppressed [48]. Details of the simulations are given in the appendix.

Starting with head-on collisions, we show how the distribution of $\chi_{\rm max}$, the largest quantum parameter attained by the electron on its passage through the laser pulse, is affected by the duration of a linearly polarised, plane-wave laser pulse. The electron initial Lorentz factor γ_0 is set to be one of 5×10^3, 2×10^4, and 10^5. The laser a_0 is chosen such that χ_0 is 1, 10 and 100 respectively. The laser frequency is fixed at $\omega_0 = 1.55$ eV and the pulse duration τ is varied from 2 to 200 wavelengths. The distributions of $\chi_{\rm max}$ shown in figure 1 demonstrate that increasing the pulse duration strongly reduces the number of electrons that reach large quantum parameter. This behaviour is captured by (4), which we find to be a good quantitative prediction of the 90th percentile of the distribution, provided $n_{\rm eff} \gtrsim 2$. Otherwise the specific value of the carrier envelope phase $\phi_{\rm CEP}$ must be taken into account [49], as the maximal electric field of a pulse $E(\phi) \propto a(\phi)\sin(\phi + \phi_{\rm CEP})$ is smaller for $\phi_{\rm CEP} = 0$ than $\phi_{\rm CEP} = \pi/2$, and the difference grows as the duration is reduced. We set $\phi_0 = 0$ throughout this paper,

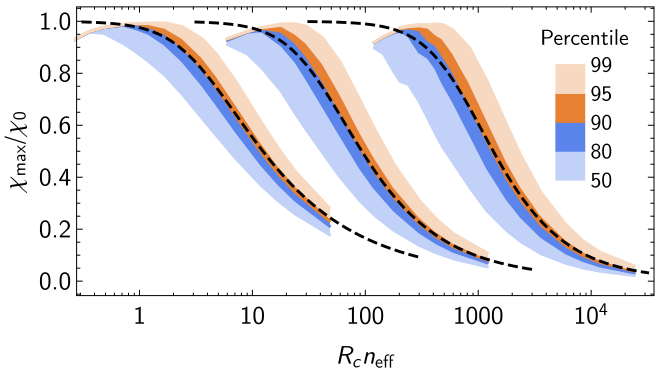

Figure 1. Radiation reaction limits the maximum quantum parameter reached by the electron χ_{max}: the distribution of χ_{max} reached in a laser-electron collision where the largest possible $\chi_e = \chi_0$ is (colour scale, left to right) 1, 10 and 100 from simulations and (dashed lines) our analytical prediction of the same, (4). See text for other collision parameters.

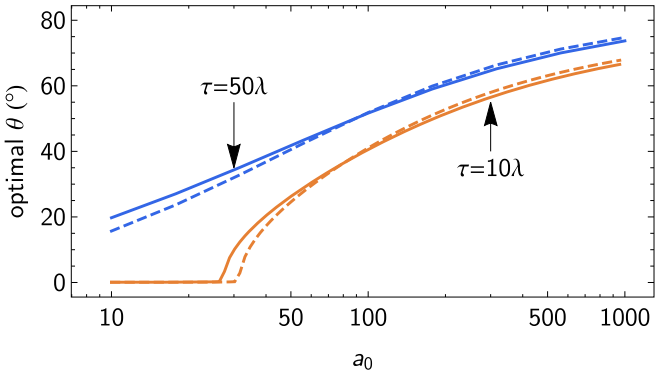

Figure 2. The angle at which χ_{max} is largest, as predicted by (4): for a collision between an electron beam with $\gamma_0 = 2 \times 10^4$ (solid) and 5×10^3 (dashed) and a laser pulse with given a_0, wavelength $\lambda = 0.8$ μm, spot size $r_0 = 2$ μm and duration $\tau = 50\lambda$ (blue) and 10λ (orange).

which is why the upper bounds of the distributions shown in figure 1 roll over as $R_c n_{eff}$ is reduced. They would saturate at $\chi_{max} = \chi_0$ if instead $\phi_0 = \pi/2$.

Equation (4) can be solved to find the largest laser pulse duration τ for which $\chi_{max} > \chi_0/2$. We find that $\tau \lesssim 8m\gamma_0/\mathcal{P}(\chi_0/2)$, where $\mathcal{P}$ the radiated power (including quantum corrections) of an electron with given χ. The larger the radiated power, the shorter the pulse must be to ensure that at least 10% of the electrons reach a quantum parameter of at least $\chi_0/2$. For the three cases shown in figure 1, we predict the duration τ can be at most 137, 41.2 and 30.0 fs before this happens, in good agreement with the simulation results where the largest τ is 131, 41.7 and 30.1 fs respectively.

3. Enhanced signatures of quantum effects

Equation (1) leads us to expect that quantum effects are strongest in the head-on collision geometry, where the geometric factor $1 + \cos\theta$ is largest. However, unless the pulse duration is as little as a few cycles in length (when radiation 'quenching' is possible [44]), radiation reaction strongly reduces the number of electrons that get close to the maximum possible χ_e. This can be mitigated by moving to collisions at oblique incidence, because the spot to which a laser pulse is focussed ($\sim$2 μm) is typically smaller than the length of its temporal profile (20 fs [31], 30 fs [29, 30, 33] or 150 fs [32]). Even though the maximum possible χ_e at $\theta > 0$ is smaller than that at $\theta = 0$, many more electrons get close to the maximum because the interaction length is shorter and radiative losses are reduced. This is illustrated in figure 2, where the collision angle θ, predicted by (4) to maximise χ_{max}, is plotted for two exemplary pulse durations $\tau = 10\lambda$ and 50λ (27 and 130 fs respectively at a wavelength of 0.8 μm). The shorter the pulse duration, the larger a_0 can be before the head-on collision ceases to be optimal. As the laser amplitude is increased, radiation reaction becomes stronger and the optimal angle increases away from zero. The increased χ_{max} at oblique incidence enhances two quantum effects: the emission of photons with energy comparable to that of the electron, and the stochastic broadening of the electron energy spectrum.

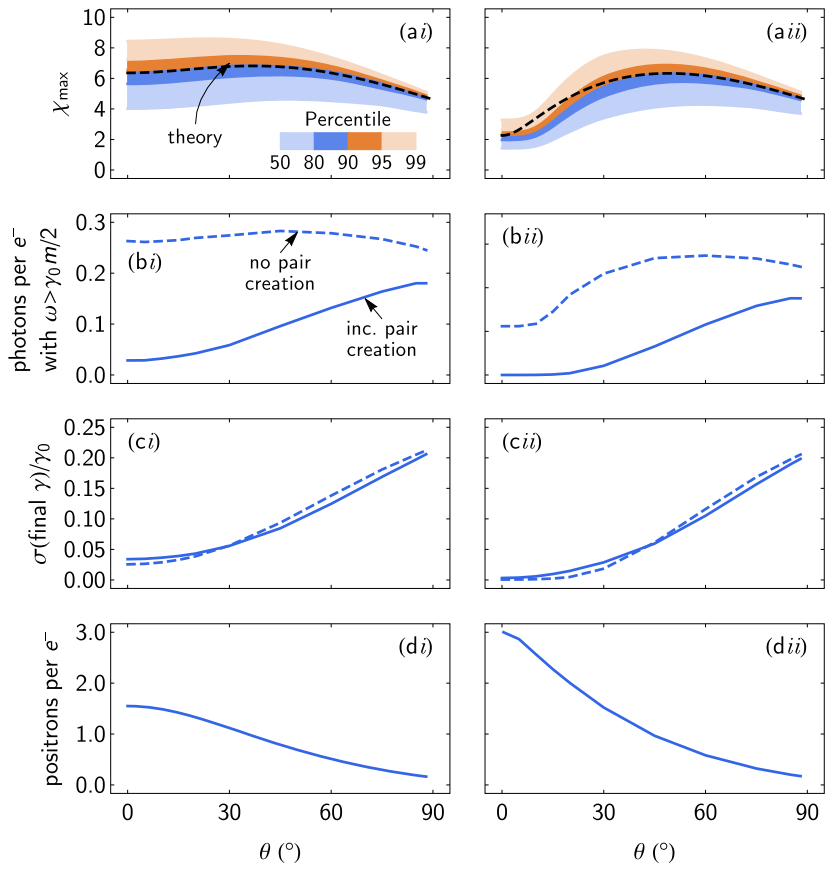

Figure 3. Enhanced quantum effects at oblique incidence: (a) distribution of χ_{max}; (b) the number of photons per electron with energy $\omega > \gamma_0 m/2$; (c) the standard deviation of the final γ; and (d) the number of positrons per electron, after electrons with $\gamma_0 = 2 \times 10^4$ collide at angle θ with a laser pulse with $a_0 = 82.4$, wavelength $\lambda = 0.8$ μm, focal spot size $r_0 = 2$ μm and a duration of (i) $\tau = 10\lambda$ and (ii) 50λ. In (b), (c) results are from simulations with (solid) and without (dashed) electron–positron pair creation.

In figure 3 we show how these two signatures are affected by the collision angle θ in a QED cascade when $\chi_0 = 10$ and the laser pulse duration is one of $\tau = 10\lambda$ and 50λ. As the (linearly polarised) laser is focussed tightly to a spot size of $r_0 = 2$ μm, the electromagnetic field in our simulations is calculated up to fourth-order in the diffraction angle $\epsilon = r_0 / z_R$ where $z_R = \pi r_0^2 / \lambda$ is the Rayleigh range [40]. Further details of the simulations are given in the appendix. The dependence of the distribution of χ_{max} on the angle is different in the two cases: whereas it is approximately constant at $\chi_{max} \simeq 5$ for the shorter pulse, the maximum quantum parameter is strongly suppressed for $\theta < 15°$ for the longer pulse. We find that not only is χ_{max} maximised at $\theta \simeq 45°$ rather than at 0°, as shown in figure 2, but that the value at 90° is twice that at 0°. The reduced apparent pulse duration at normal incidence more than compensates for the reduction in the geometric factor in χ_e because it reduces the electron's total loss of energy to radiation. Our theoretical scaling (4) captures both these effects, in close agreement with the simulation results.

The number of high-energy photons is especially sensitive to the highest χ_e reached by the electron [24, 43]. Accordingly, consider the number of photons N_γ with energy $\omega > \gamma_0 m/2$ in the absence of electron–positron pair creation (the dashed lines in figure 3(b)). For the shorter pulse, N_γ is almost independent of the collision angle, whereas for the longer pulse, it is maximised at $\theta \simeq 45°$ and suppressed for $\theta < 15°$ [50]. In both cases the dependence of N_γ on θ mimics that of χ_{max}. When depletion of the photon spectrum due to electron–positron pair creation is included, the optimal angle is increased to 90° for both pulse durations. This is because the reduced interaction length at normal incidence suppresses the pair creation probability [39], as shown in figure 3(d).

Another important signature of quantum effects on radiation reaction is broadening of the electron energy spectrum [25], caused by the stochasticity of photon emission [23]. The variance of the energy distribution σ_γ^2 is studied in detail in [51–54], where it is shown that the temporal evolution of the variance is governed by two competing terms: one that arises because the radiated power is larger for higher energy electrons, which favours decreasing σ_γ, and a stochastic term, which favours increasing σ_γ. The broadening term dominates if χ_e is large and the pulse duration is short. Both of these cause oblique incidence to be favoured for the scenario explored in figure 3: χ_{max} is larger at $\theta > 0$ (or at least, not significantly reduced) and the interaction length is shorter as well.

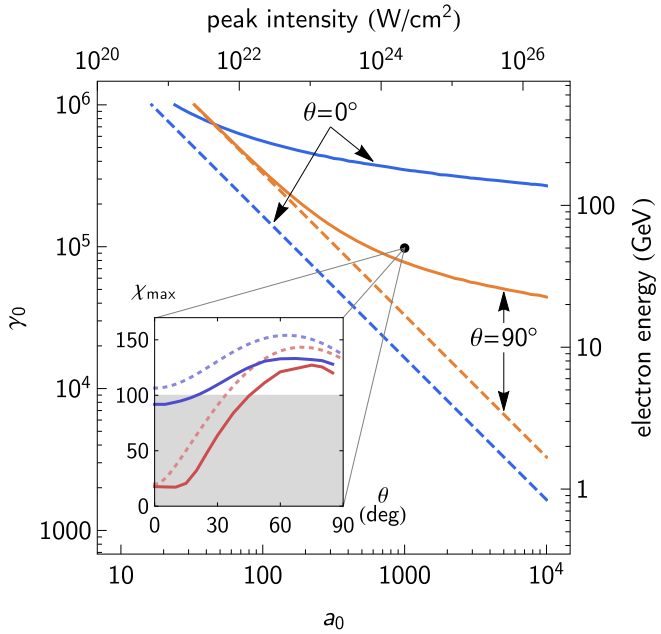

Figure 4. The minimum γ_0 and a_0 required for $\chi_e \geqslant 100$ ($\alpha\chi_e^{2/3} \geqslant 0.16$): we compare (1) (dashed lines), which neglects radiative losses, with (4), which includes them, for an electron colliding with a linearly polarised laser pulse (wavelength $\lambda = 0.8$ μm, duration $\tau = 50\lambda$ and focal spot size $r_0 = 2$ μm). We see that collisions at normal incidence (orange) are very strongly favoured over head-on (blue) when radiative losses are accounted for. (inset) Theoretical χ_{max} (4) (dashed) and the 90th percentile of the χ_{max} distribution from simulations (solid) as a function of angle θ for a collision at 50 GeV and $a_0 = 1000$ for pulse duration of 10λ(purple) and 50λ (red).

Figure 3(c) shows that the variance of the post-collision energy is larger for larger θ [55], and that this is not changed appreciably by electron–positron pair creation.

4. Towards radiative corrections in strong-field QED

We now consider the collision parameters necessary to reach $\alpha\chi_e^{2/3} \gtrsim 1$, where strong-field QED is conjectured to become fully nonperturbative. By this we mean that perturbation theory with respect to the dynamical electromagnetic field breaks down [17]: for example, the lowest order correction to the strong-field QED vertex $V_\mu^{(1)} = ie\gamma_\mu$ grows as $V^{(3)} \sim \alpha\chi_e^{2/3} V^{(1)}$ [56] (debated in [57]). Recall that the theory is already nonperturbative in the sense that amplitudes must be calculated to all orders in coupling to the background electromagnetic field a_0 if $a_0 > 1$ [8]. The qualitative difference from perturbative QED is that radiative corrections are expected to grow as power laws, rather than logarithmically, in the strong-field regime [18] (the transition between the two is studied in [58, 59]).

Reaching such large χ_e is therefore of fundamental interest, but experimentally challenging. The obstacle is severe radiation losses at large χ_e: in the case where the strong field is provided by a tightly focussed, ultraintense laser, we show how the collision angle plays an important role in mitigating these losses by reducing the interaction time. In the beam–beam geometry Yakimenko *et al* [60] propose to reach $\alpha\chi_e^{2/3} \sim 1$, the electron-bunch length plays the important role; in an alternative geometry of laser-electron-beam collision proposed by Baumann *et al* [61], the interaction time is reduced by plasma-based compression of a single-cycle laser pulse to sub-femtosecond duration, in advance of the collision. Strictly the calculation cannot be done for $\alpha\chi_e^{2/3} \sim 1$, because we would need all the radiative corrections; however, we can estimate when they become significant by using our results to find the collision parameters necessary to reach, say, $\chi_e = 100$, at which the vertex correction is of order 10% and radiative corrections begin to become non-negligible. Note that the energy loss which reduces χ_{max} from χ_0 occurs within the intensity ramp where radiative corrections are less important. Hence, while our analysis neglects such corrections, the crucial physical insight remains accurate.

The dashed lines in figure 4 show the minimum γ_0 and a_0 if χ_e were given by (1): it is evident that the ideal collision angle $\theta = 0$. This is no longer the case when dynamical effects are taken into account. Using (4) to estimate the minimum energy and laser intensity instead, we find that collisions at $\theta = \pi/2$ are strongly favoured for a pulse with duration $\tau = 50\lambda$. The additional electron energy or laser intensity necessary to compensate radiative losses can be substantial, which is indicated by the vertical (horizontal) gaps between the solid and dashed lines. At $a_0 = 1000$ and $\theta = 0$, for example, the minimum energy must be increased by more

than an order of magnitude, from the naive estimate of 8.4–180 GeV. The gradient of the lines indicates that the necessary increase in γ_0 is always smaller than the equivalent increase in a_0. As discussed earlier, this is because of the stronger dependence of the photon emission rate on a_0.

At $a_0 = 1000$, which is equivalent to an intensity of 2×10^{24} W cm^{-2} at a wavelength of 0.8 μm, the energy required to reach $\chi_e = 100$ and the onset of radiative corrections is ~ 40 GeV, at which point oblique incidence is favoured for both $\tau = 10\lambda$ and 50λ (see inset of figure 4). This energy is readily achievable with conventional accelerators [6, 7] and the necessary laser system is of the kind being commissioned at the ELI facilities [26]. The required laser intensity may be reduced at the expense of increasing the electron beam energy; according to figure 2, this reduces the optimal angle of incidence, whereas tighter focussing, i.e. reduction of r_0, would cause it to increase. It is important to note that the laser intensity cannot be reduced to an arbitrarily low level, and the electron energy increased to compensate, because power-law growth of the radiative corrections occurs only in the high-intensity limit $a_0 \gg 1$; if $\alpha\chi_e^{2/3} \gtrsim 0.1$ is approached by means of ever higher electron energies instead, that growth would be logarithmic as in perturbative QED [58, 59].

$\chi_{\max}$ increases as r_0 becomes smaller, assuming oblique incidence and fixed a_0. Tighter focussing is therefore motivated, not only to achieve the highest possible intensity, but also to reduce radiative energy losses. This can also be interpreted as a minimal requirement on the quality of the focussing. 'Wings' around the focal spot would increase the interaction time, which effectively increases the spot size r_0 in (4). Consider, for example, the collision of a 50 GeV electron beam with a pulse that has radial profile $a(r) = a_0[(1-\delta)\mathrm{e}^{-r^2/r_0^2} + \delta\mathrm{e}^{-r^2/(fr_0)^2}]$ at oblique incidence $\theta = 85°$. We set $\delta = 0.1$, $r_0 = 2$ μm and increase f from 1 to 2, causing a shoulder to develop in the intensity profile at the focal plane. The increased interaction time increases the energy loss of the electron beam and reduces the maximum χ_e reached: simulations indicate that at $\chi_0 = 1000$, the 90th percentile of $\chi_{\max}$ is reduced by 15%, from $0.13\chi_0$ to $0.11\chi_0$. Increasing r_0 from 2 to 2.55 μm would, according to (4), cause the same decrease and therefore the latter may be regarded as an *effective* focal spot size for the modified radial profile. An extension of (4) for more general radial and temporal intensity profiles will be addressed in future work.

Alignment of the beams is, admittedly, more challenging at oblique incidence than it is for head-on collisions, which has been the focus of previous experimental work on radiation reaction [27, 28]. Nevertheless, an argument in its favour that the initial beam and its collision products are directed well away from the laser focussing optic. Furthermore, if the laser pulse is sufficiently intense or long that radiation reaction would suppress $\chi_{\max}$ well below the χ_e necessary to observe the onset of radiative corrections, then regardless of whether the beams overlap or not, the collision will be unsuccessful in reaching the regime in question. Our results, including (4), can be used to determine whether it is possible for a particular set of collision parameters. Successful overlap between the beams can be identified by means of coincidence measurements of the γ-ray flash, the electron energy loss and positron production, because as figure 3 shows, the numbers of high-energy photons and positrons are sensitive to the highest χ_e reached and the duration over which it is sustained.

5. Summary

We have studied how to reach large quantum parameter in the collision of an electron beam with an intense laser pulse. Our scaling for the maximum χ_e, which is verified by Monte Carlo simulations, predicts that the optimal collision geometry is not head-on for long or high-intensity laser pulses. This is because of strong radiative losses, which reduce the electron energy and so its quantum parameter. The growth of χ_e is then much weaker than the linear scaling of the naive prediction, which ignores radiation losses and thereby overestimates the efficiency of χ_e-generation. The shorter interaction length at oblique incidence compensates for the geometric reduction in χ_e, causing signatures of quantum effects to be enhanced at $\chi_e = 10$. Beyond their applicability to nearer term experiments, our results show that a collision at oblique incidence is a viable platform for studying the onset of the breakdown of perturbative strong-field QED at $\alpha\chi_e^{2/3} \gtrsim 0.1$. It is be to hoped that the feasibility of reaching this regime in a future high-intensity laser experiment will further motivate the theoretical work necessary to identify its explicit signatures, and how modifications to the photon emission and pair creation rates manifest themselves.

Acknowledgments

The authors acknowledge support from the Knut and Alice Wallenberg Foundation (TGB and MM), the Swedish Research Council (grants 2013-4248 and 2016-03329, MM) and the Engineering and Physical Sciences Research Council (grant EP/M018156/1, CPR). Simulations were performed on resources provided by the Swedish National Infrastructure for Computing (SNIC) at the High Performance Computing Centre North (HPC2N).

Appendix. Monte Carlo simulations

In this appendix, we summarise the method by which the interaction between electrons and intense lasers can be modelled in the quantum radiation reaction regime.

In the semiclassical approach to the collision process, the electron follows a (radiation-free) classical trajectory between point-like, probabilistically determined, QED events. These events are implemented using the standard Monte Carlo algorithm [46, 47], with rates calculated in the locally constant field approximation [8, 9]. We use `circe`, a particle-tracking code that simulates photon and positron production by high-energy electrons and photons in intense laser pulses. Collective effects and back-reaction on the external field are neglected, as appropriate for the charge densities under consideration here. In between emissions, the particle trajectories follow from the Lorentz force equation. If the external field is a plane wave, the particle push takes the following form [62]: the spatial components of the momentum p^μ perpendicular to the laser wavevector k are determined by $\partial_\phi \vec{p}_\perp = -e\vec{E}_\perp(\phi)/\omega_0$, where $\vec{E}_\perp$ is the electric field at phase ϕ and the angular frequency $\omega_0 = k^0$. The other two components follow from the conditions $k.p = \text{const}$ and $p^2 = m^2$, and the position from $\partial_\phi x^\mu = p^\mu/k.p$. If the field is a focussed Gaussian beam, and therefore a function of all three spatial coordinates, we use the particle push introduced by Vay [63] and the analytical expressions given in [40].

To model photon emission, each electron is initialised with an optical depth against emission $\tau = -\log(1-R)$ for pseudorandom $0 \leqslant R < 1$, which evolves as $\partial_t \tau = W(\chi_e, \gamma)$, where $W(\chi_e, \gamma)$ is the instantaneous probability rate of emission, χ_e the electron quantum parameter and γ its Lorentz factor, until the point where τ falls below zero. Then the energy of the photon is pseudorandomly sampled from the differential spectrum and τ is reset. We assume that emission occurs in the direction parallel to the initial momentum, as the electron emits into a narrow cone of opening angle $1/\gamma$, which determines the electron momentum after the scattering by the conservation of momentum. The most stringent restriction on the timestep Δt at high intensity is that the probability of multiple emissions per step be much smaller than 1, i.e. $\Delta\tau \ll 1$. The timestep is then determined by $\Delta\tau \simeq 1.44\alpha\chi_0\Delta t/\gamma_0 \leqslant 10^{-2}$, or $\omega_0\Delta t/(2\pi) \leqslant 10^{-2}$, whichever leads to the smaller result. Electron–positron pair creation by photons is modelled in an analogous way, except the photons follow a ballistic trajectory from their point of creation, and on the creation of the pair, the parent photon is deleted from the simulation. At least 10^6 electrons are used per simulation to generate sufficient statistics.

ORCID iDs

T G Blackburn https://orcid.org/0000-0002-3681-356X
A Ilderton https://orcid.org/0000-0002-6520-7323
M Marklund https://orcid.org/0000-0001-9051-6243
C P Ridgers https://orcid.org/0000-0002-4078-0887

References

[1] Sauter F 1931 *Z. Phys.* **69** 742
[2] Schwinger J 1951 *Phys. Rev.* **82** 664–79
[3] Mourou G A, Tajima T and Bulanov S V 2006 *Rev. Mod. Phys.* **78** 309–71
[4] Marklund M and Shukla P K 2006 *Rev. Mod. Phys.* **78** 591–640
[5] Di Piazza A, Müller C, Hatsagortsyan K Z and Keitel C H 2012 *Rev. Mod. Phys.* **84** 1177–228
[6] Bula C *et al* 1996 *Phys. Rev. Lett.* **76** 3116–9
[7] Burke D L *et al* 1997 *Phys. Rev. Lett.* **79** 1626–9
[8] Ritus V I 1985 *J. Sov. Laser Res.* **6** 497–617
[9] Erber T 1966 *Rev. Mod. Phys.* **38** 626–59
[10] Sokolov I V, Naumova N M, Nees J A and Mourou G A 2010 *Phys. Rev. Lett.* **105** 195005
[11] Bulanov S S, Schroeder C B, Esarey E and Leemans W P 2013 *Phys. Rev.* A **87** 062110
[12] Harding A K and Lai D 2006 *Rep. Prog. Phys.* **69** 2631
[13] Ruffini R, Vereshchagin G and Xue S S 2010 *Phys. Rep.* **487** 1–140
[14] Timokhin A N and Harding A K 2015 *Astrophys. J.* **810** 144
[15] Bell A R and Kirk J G 2008 *Phys. Rev. Lett.* **101** 200403
[16] Ridgers C P, Brady C S, Duclous R, Kirk J G, Bennett K, Arber T D, Robinson A P L and Bell A R 2012 *Phys. Rev. Lett.* **108** 165006
[17] Narozhny N B 1980 *Phys. Rev.* D **21** 1176–83
[18] Fedotov A M 2017 *J. Phys.: Conf. Ser.* **826** 012027
[19] Bulanov S V, Esirkepov T Z, Koga J and Tajima T 2004 *Plasma Phys. Rep.* **30** 196–213
[20] Koga J, Esirkepov T Z and Bulanov S V 2005 *Phys. Plasmas* **12** 093106
[21] Hadad Y, Labun L, Rafelski J, Elkina N, Klier C and Ruhl H 2010 *Phys. Rev.* D **82** 096012
[22] Kravets Y, Noble A and Jaroszynski D 2013 *Phys. Rev.* E **88** 011201
[23] Shen C S and White D 1972 *Phys. Rev. Lett.* **28** 455–9
[24] Blackburn T G, Ridgers C P, Kirk J G and Bell A R 2014 *Phys. Rev. Lett.* **112** 015001
[25] Neitz N and Di Piazza A 2013 *Phys. Rev. Lett.* **111** 054802

[26] Turcu I et al 2016 Rom. Rep. Phys. 68 S145–231
[27] Cole J M et al 2018 Phys. Rev. X 8 011020
[28] Poder K et al 2018 Phys. Rev. X 8 031004
[29] Bahk S W, Rousseau P, Planchon T A, Chvykov V, Kalintchenko G, Maksimchuk A, Mourou G A and Yanovsky V 2004 Opt. Lett. 29 2837–9
[30] Pirozhkov A S et al 2017 Opt. Express 25 20486–501
[31] Papadopoulos D et al 2016 High Power Laser Sci. Eng. 4 e34
[32] Weber S et al 2017 Matter Radiat. Extremes 2 149–76
[33] Gales S et al 2018 Rep. Prog. Phys. 81 094301
[34] Uggerhøj U I 2005 Rev. Mod. Phys. 77 1131–71
[35] Wistisen T N, Di Piazza A, Knudsen H V and Uggerhøj U I 2018 Nat. Commun. 9 795
[36] Kirsebom K, Mikkelsen U, Uggerhøj E, Elsener K, Ballestrero S, Sona P and Vilakazi Z Z 2001 Phys. Rev. Lett. 87 054801
[37] Chen P and Telnov V I 1989 Phys. Rev. Lett. 63 1796–9
[38] Esberg J, Uggerhøj U I, Dalena B and Schulte D 2014 Phys. Rev. ST Accel. Beams 17 051003
[39] Blackburn T G, Ilderton A, Murphy C D and Marklund M 2017 Phys. Rev. A 96 022128
[40] Salamin Y I 2007 Appl. Phys. B 86 319–26
[41] Li J X, Hatsagortsyan K Z, Galow B J and Keitel C H 2015 Phys. Rev. Lett. 115 204801
[42] Blackburn T G and Marklund M 2018 Plasma Phys. Control. Fusion 60 054009
[43] Duclous R, Kirk J G and Bell A R 2011 Plasma Phys. Control. Fusion 53 015009
[44] Harvey C N, Gonoskov A, Ilderton A and Marklund M 2017 Phys. Rev. Lett. 118 105004
[45] Di Piazza A, Hatsagortsyan K Z and Keitel C H 2010 Phys. Rev. Lett. 105 220403
[46] Ridgers C P, Kirk J G, Duclous R, Blackburn T G, Brady C S, Bennett K, Arber T D and Bell A R 2014 J. Comput. Phys. 260 273–85
[47] Gonoskov A, Bastrakov S, Efimenko E, Ilderton A, Marklund M, Meyerov I, Muraviev A, Sergeev A, Surmin I and Wallin E 2015 Phys. Rev. E 92 023305
[48] Dinu V, Harvey C, Ilderton A, Marklund M and Torgrimsson G 2016 Phys. Rev. Lett. 116 044801
[49] Mackenroth F, Di Piazza A and Keitel C H 2010 Phys. Rev. Lett. 105 063903
[50] Blackburn T G 2015 Plasma Phys. Control. Fusion 57 075012
[51] Yoffe S R, Kravets Y, Noble A and Jaroszynski D A 2015 New J. Phys. 17 053025
[52] Vranic M, Grismayer T, Fonseca R A and Silva L O 2016 New J. Phys. 18 073035
[53] Ridgers C P et al 2017 J. Plasma Phys. 83 715830502
[54] Niel F, Riconda C, Amiranoff F, Duclous R and Grech M 2018 Phys. Rev. E 97 043209
[55] Yoffe S R, Noble A, Macleod A J and Jaroszynski D A 2017 Proc. SPIE 10234 102340E
[56] Morozov D A, Narozhnyi N B and Ritus V I 1981 Sov. Phys.—JETP 53 1103
[57] Gusynin V P, Miransky V A and Shovkovy I A 1999 Nucl. Phys. B 563 361–89
[58] Podszus T and Di Piazza A 2019 Phys. Rev. D 99 076004
[59] Ilderton A 2019 Phys. Rev. D 99 085002
[60] Yakimenko V et al 2018 arXiv:1807.09271
[61] Baumann C, Nerush E N, Pukhov A and Kostyukov I Y 2018 arXiv:1811.03990
[62] Blackburn T G, Seipt D, Bulanov S S and Marklund M 2018 Phys. Plasmas 25 083108
[63] Vay J L 2008 Phys. Plasmas 15 056701